

Electronic Supplementary Material (ESI) for Journal of Materials Chemistry A.

Electronic Supplementary Information

Honeycomb-layer structured $\text{Na}_3\text{Ni}_2\text{BiO}_6$ as a high voltage and long life cathode material for sodium-ion batteries

Deu S. Bhang, ^{a,b,‡} Ghulam Ali, ^{c,d,‡} Dong-Hyun Kim, ^c Daniel A. Anang, ^a Tae Joo Shin, ^e Min-Gyu Kim, ^f Yong-Mook Kang^a, Kyung-Yoon Chung^{c,d*} and Kyung-Wan Nam^{a*}

^a *Department of Energy and Materials Engineering, Dongguk University-Seoul, 04620 Seoul, Republic of Korea, Email: knam@dongguk.edu*

^b *Department of Chemistry, Shivaji University, Kolhapur 416004, India*

^c *Center for Energy Convergence Research, Korea Institute of Science and Technology, Seoul 02792, Republic of Korea, E-mail: kychung@kist.re.kr*

^d *Korea University of Science and Technology, 217 Gajeong-ro, Yuseong-gu, Daejeon 34113, Republic of Korea*

^e *UNIST Central Research Facilities & School of Natural Science, Ulsan National Institute of Science and Technology (UNIST), Ulsan 44919, Republic of Korea*

^f *Pohang Accelerator Laboratory (PAL), Pohang 790-784, Republic of Korea*

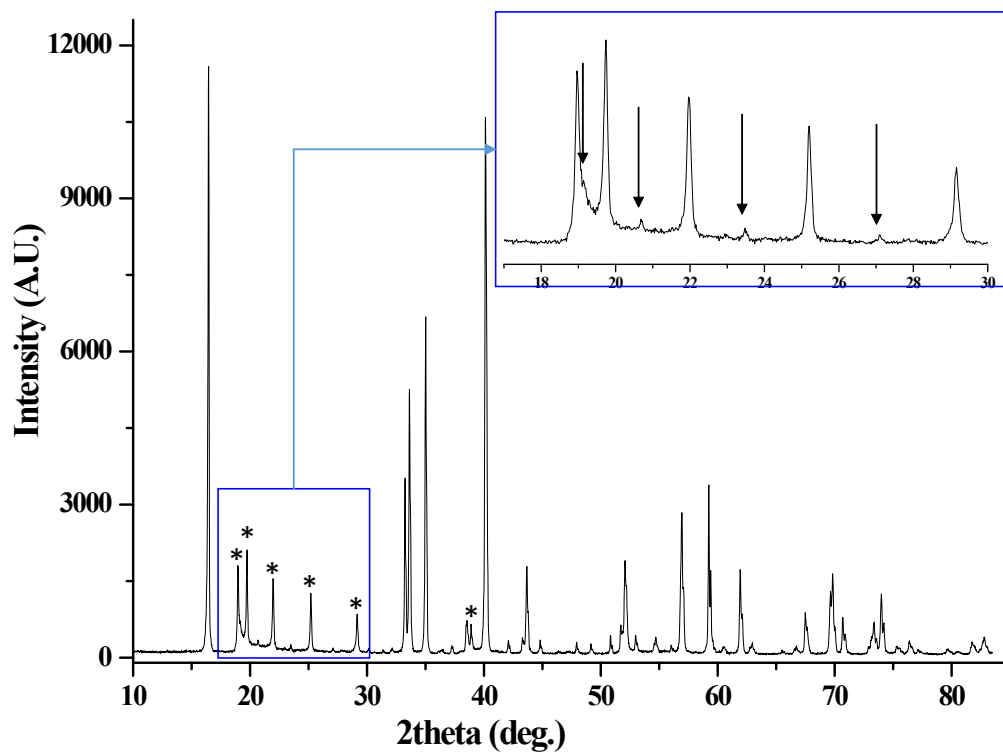


Fig. S1 Laboratory powder XRD pattern ($\lambda=1.5406\text{\AA}$) of $\text{Na}_3\text{Ni}_2\text{BiO}_6$ prepared in this study using solid-state reaction. Asterisk marks are used to highlight the super-structure reflections. Inset shows the expanded view in the 2θ region between 17 and 30° to better represent additional weak reflections (marked by arrows) due to $C2/c$ symmetry ($\lambda=1.5406\text{ \AA}$).

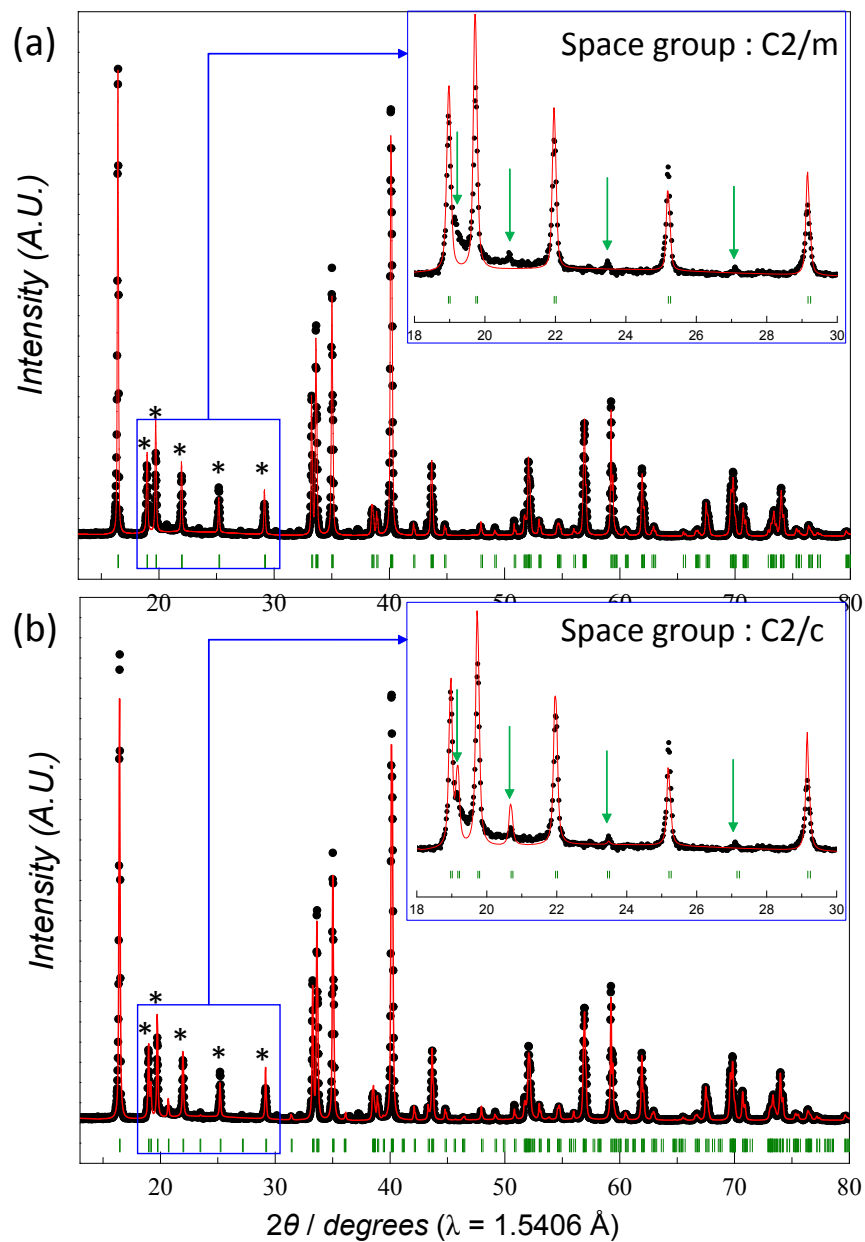


Fig. S2 Le Bail fit of the Laboratory XRD pattern with (a) $C2/m$ and (b) $C2/c$ symmetry for the $\text{Na}_3\text{Ni}_2\text{BiO}_6$. Insets show the expanded view of the super-structure peaks in the 2θ range between 17 to 30° to show the presence of weakly intense reflections (marked by green arrows).

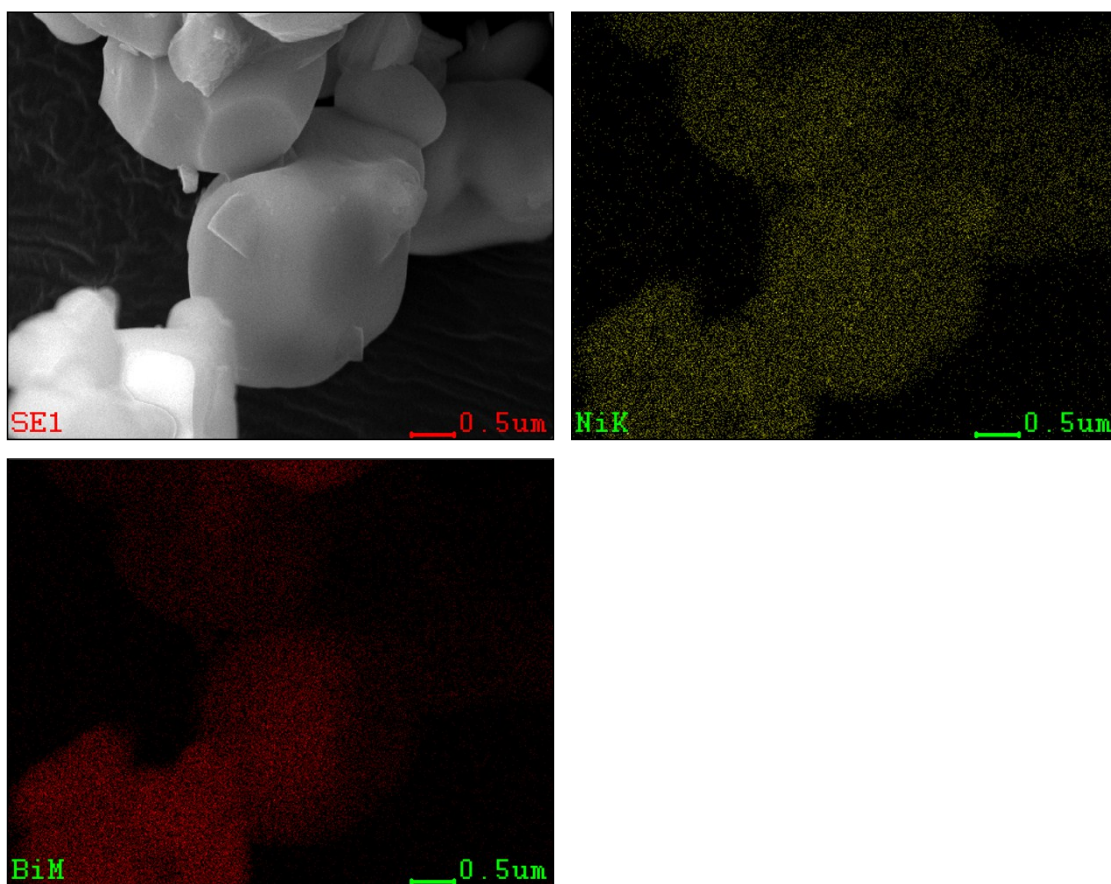


Fig. S3 Elemental mapping of the Ni and Bi throughout the sample of $\text{Na}_3\text{Ni}_2\text{BiO}_6$ using characteristic X-rays.

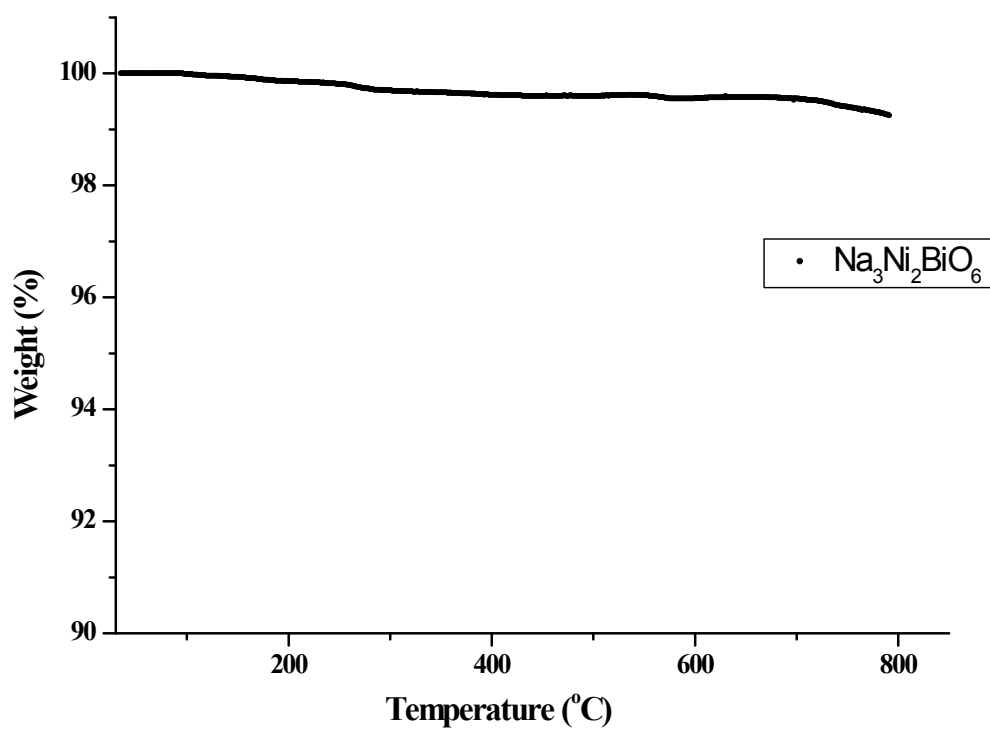


Fig. S4 TGA curve of the Na₃Ni₂BiO₆ powder exposed to ambient air atmosphere.

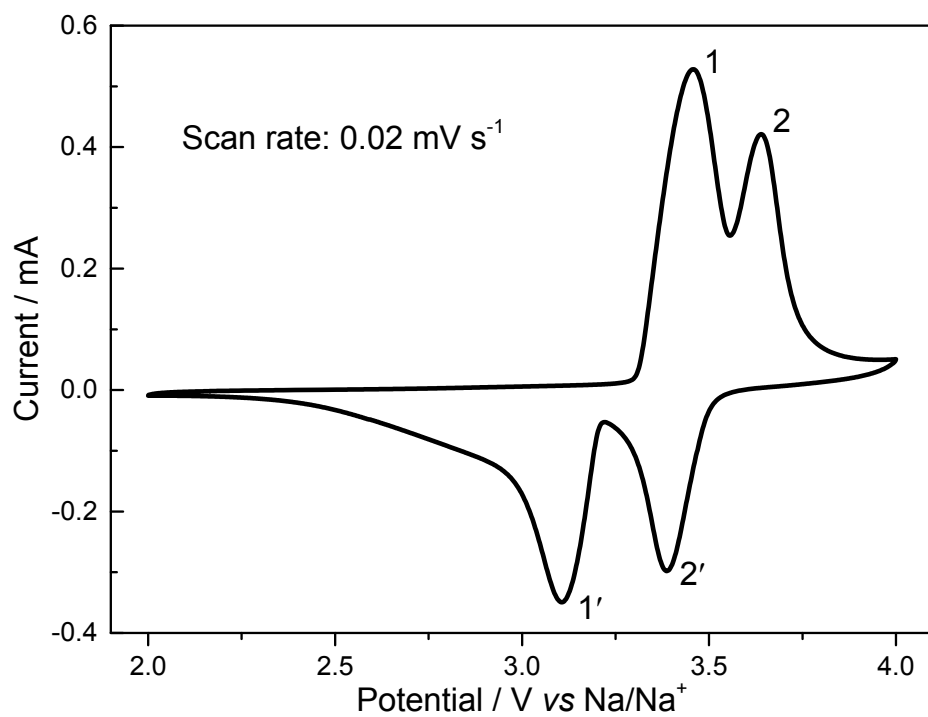


Fig. S5 Cyclic voltammogram (CV) profile of the Na₃Ni₂BiO₆ electrode at a scan rate of 0.02 mV s⁻¹.

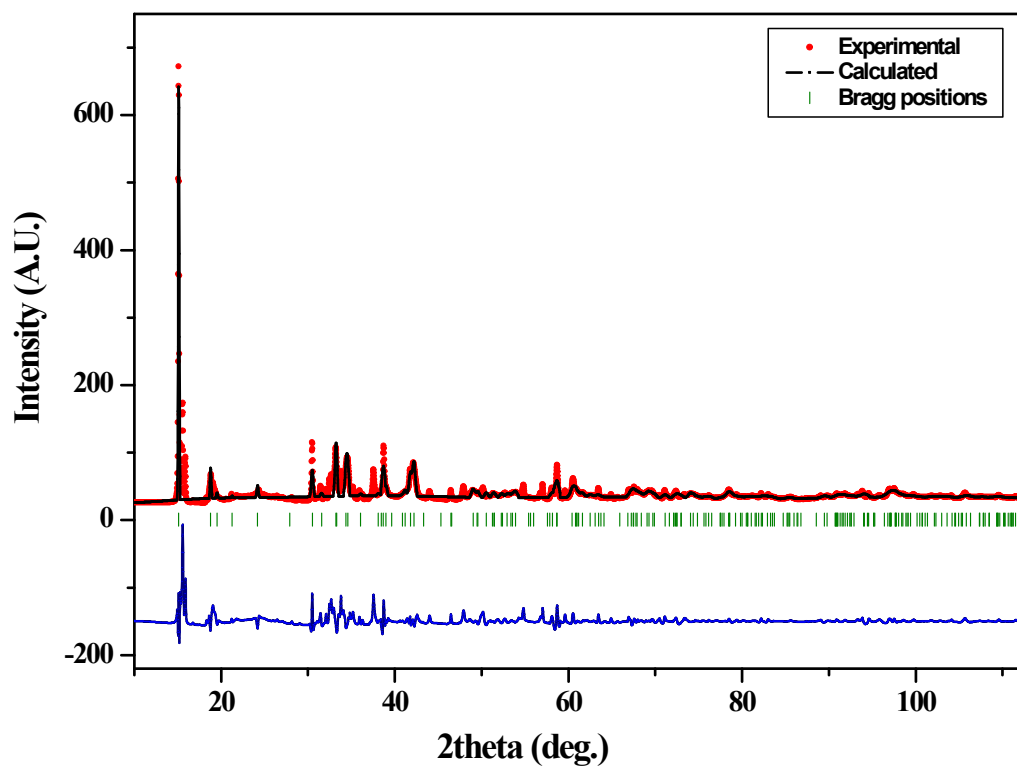


Fig. S6 Le Bail fit for the intermediate charged (3.4V) $\text{Na}_3\text{Ni}_2\text{BiO}_6$, equivalent to extraction of 1 Na ion from the structure (composition corresponding to $\text{Na}_2\text{Ni}_2\text{BiO}_6$).

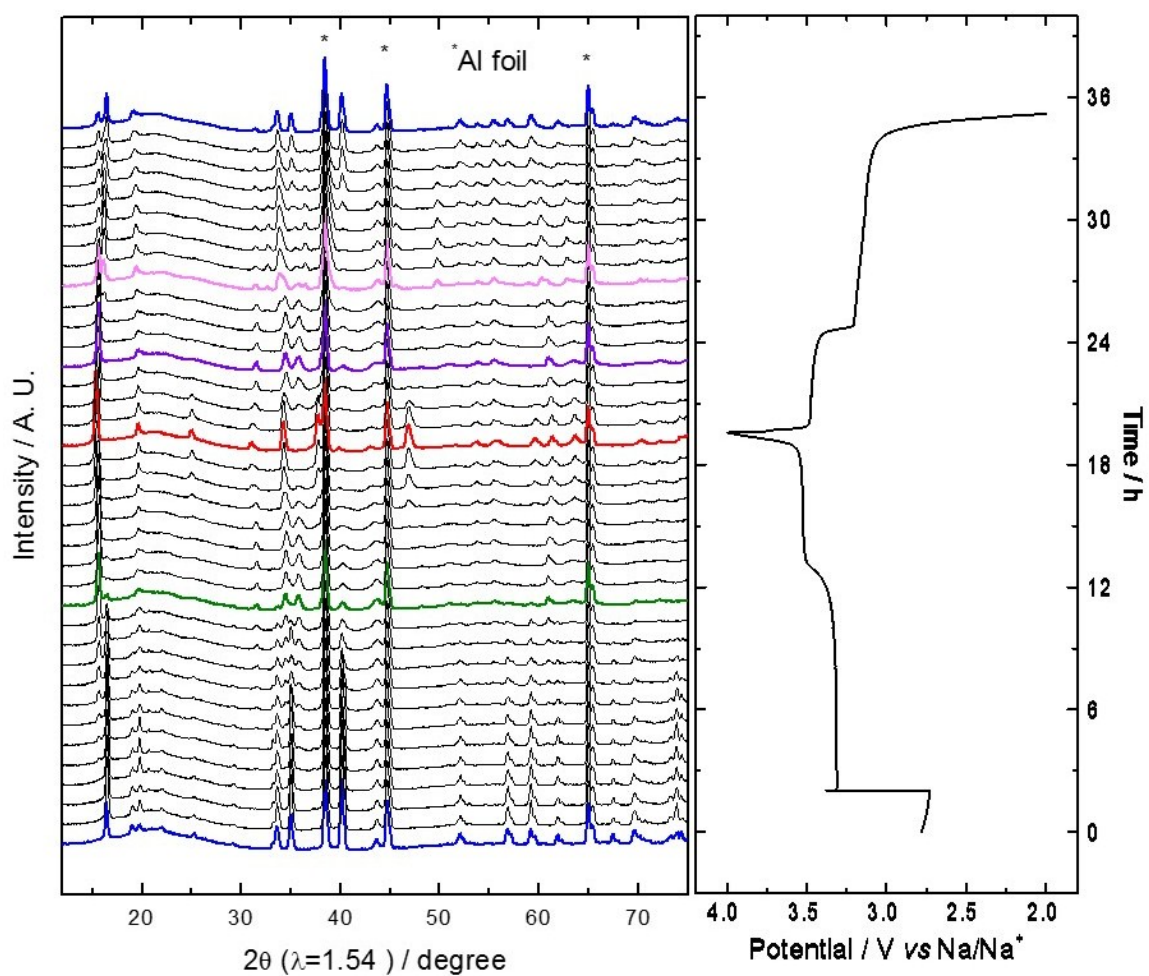


Fig. S7 (Left) In situ X-ray powder diffraction patterns collected during charging discharging of the $\text{Na}_3\text{Ni}_2\text{BiO}_6$ in the voltage of 2.0 to 4.0V. (Right) The electrochemical profile of a cell, as a function of Na content recorded during diffraction experiment. The reflection from the Al foil used for casting the electrode are marked by asterisks (*).

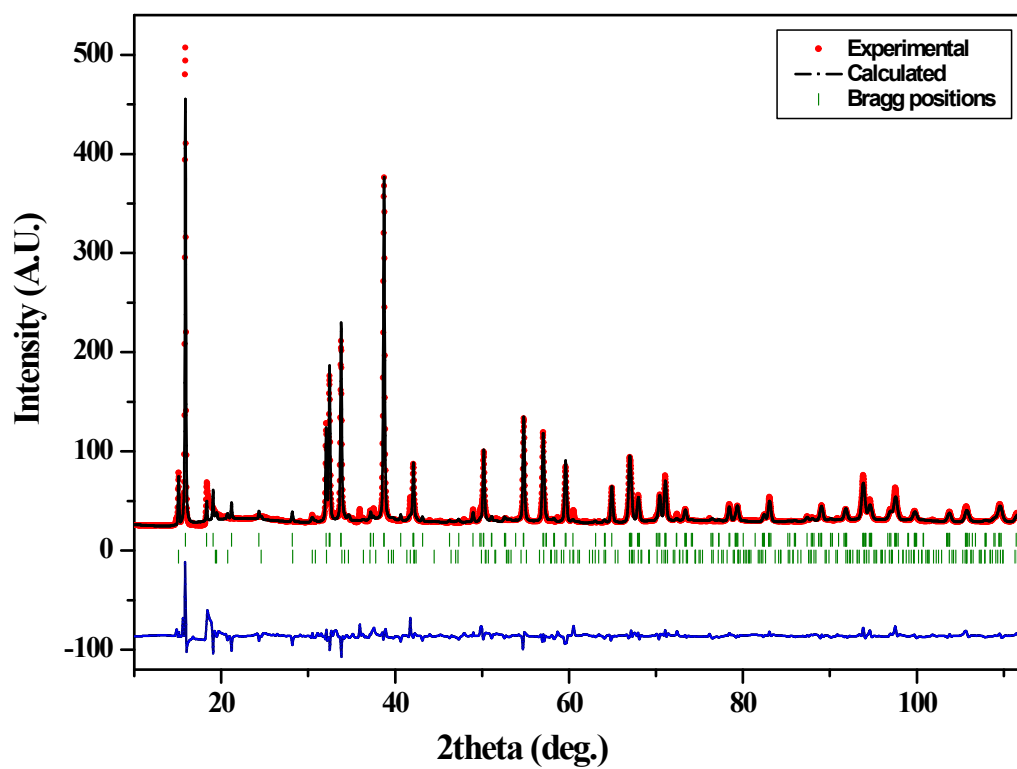


Fig. S8 Rietveld plot for the fully discharged (2V) electrode powder corresponding to chemical composition Na₃Ni₂BiO₆.

Table S1. Selected bond distances (Å) for Na₃Ni₂BiO₆ (C2/c space group).

M-O	Bond length (Å)
Na1 – O1 (x2)	2.401 (15)
Na1 – O2 (x2)	2.325 (11)
Na1 – O3 (x2)	2.435 (14)
Na2 – O1 (x2)	2.44 (2)
Na2 – O2 (x2)	2.40 (2)
Na2 – O3 (x2)	2.365 (4)
Na3 – O1 (x2)	2.461 (10)
Na3 – O2 (x2)	2.419 (15)
Na3 – O3 (x2)	2.325 (11)
<hr/>	
Ni-O1	2.101 (5)
Ni-O1	2.114 (5)
Ni-O2	2.104 (5)
Ni-O2	2.108 (5)
Ni-O3	2.101 (5)
Ni-O3	2.102 (5)
<hr/>	
Bi-O1	2.146 (3)
Bi-O2	2.146 (3)
Bi-O3	2.145 (3)

Table S2. Crystallographic data and atomic coordinates of the $\text{Na}_3\text{Ni}_2\text{BiO}_6$ (P-31 m space group) based on Rietveld refinement of synchrotron powder XRD data.

O1- $\text{NaNi}_2\text{BiO}_6$		Space group: P-31 m				
a=5.2242 (1) Å, c=5.7506 (1) Å, V=135.9 (1) Å ³						
Atom	multiplicity	x	y	z	occupancy	U _{iso}
Bi1	1	0	0	0	1	0.0064
Ni1	2	0.3333	0.6667	0	1	0.0064
O1	6	0.3525	0	0.1795	1.0	0.014
Na3	2	0.3333	0.6667	0.5	0.5	0.016

Agreement factors: R_wp=8.00%, R_p=5.18%, R_F²= 10.98%

Table S3. Selected bond distances (Å) for $\text{NaNi}_2\text{BiO}_6$ (P-31 m space group).

M-O	Bond length (Å)
Bi1 – O1	2.111 (1)
Ni1 – O1	1.983 (1)
Na1 – O1	2.503 (2)
Na2 – O1	2.44 (2)
Ni1 – Ni1	3.016 (1)

Table S4. Crystallographic data and atomic coordinates of the discharged phase of $\text{Na}_3\text{Ni}_2\text{BiO}_6$ (C2/m space group) based on Rietveld refinement of ex-situ synchrotron powder XRD data.

O3- $\text{Na}_3\text{Ni}_2\text{BiO}_6$		Space group: C2/m			
a=5.3961(3) Å, b=9.3285(6) Å, c=5.6710(2) Å, $\beta=108.493(6)^\circ$ V=270.73 (1) Å ³					
Atom	Multiplicity	x	y	z	Uiso
Bi	2	0	0	0	0.0056
Ni	4	0	0.6666	0	0.0056
O1	8	0.2299	0.8333	0.1972	0.0065
O2	4	0.2300	0.5	0.2067	0.0065
Na1	2	0	0.5	0.5	0.006
Na2	4	0.5	0.3556	0.5	0.006

Agreement factors: Rwp=6.79%, Rp=4.07%, $R_F^2=11.40\%$,

Table S5. Transformed lattice parameters of the $\text{Na}_3\text{Ni}_2\text{BiO}_6$ (pristine), $\text{Na}_2\text{Ni}_2\text{BiO}_6$ (3.4V phase) and $\text{Na}_3\text{Ni}_2\text{BiO}_6$ (at fully discharge state) in the pseudohexagonal symmetry and $\text{NaNi}_2\text{BiO}_6$ (4V phase) in hexagonal symmetry.

Lattice constants	$\text{Na}_3\text{Ni}_2\text{BiO}_6$ (pristine)	$\text{Na}_2\text{Ni}_2\text{BiO}_6$ (3.4 V)	$\text{NaNi}_2\text{BiO}_6$ (4 V)	$\text{Na}_3\text{Ni}_2\text{BiO}_6$ (discharged)
a (Å)	5.4012	5.2533	5.2242	5.3961
b (Å)	5.4008	5.2695	5.2242	5.3858
c (Å)	5.3873	5.6509	5.7506	5.3782
$\sim V$ (Å ³)	136.09	135.47	135.92	135.36

$a_{\text{mono}}=a_{\text{hex}}$; $b_{\text{mono}}=(3)^{1/2}(a_{\text{hex}})$; $c_{\text{mono}}=c_{\text{hex}}/(\sin(180-\beta))$. $\sim V=(abc)*\sin 60$

Detailed EXAFS fitting procedures;

The extracted EXAFS signal, $\chi(k)$, was weighted by k^2 to emphasize the high-energy oscillations, and then Fourier-transformed in k -ranges of 3.0 ~ 13.0 \AA^{-1} for Ni and 3.5 ~ 13.5 \AA^{-1} for Bi, using a Hanning window function to obtain the magnitude plots of the EXAFS spectra in R-space (\AA). Least-square fitting of the EXAFS spectra was performed using theoretically generated scattering paths based on the model structures. For the pristine $\text{Na}_3\text{Ni}_2\text{BiO}_6$ material, more averaged structure of C2/m space group was used instead of the structure with space group of C2/c to reduce the fitting variables. For the halfway charged ($\text{Na}_2\text{Ni}_2\text{BiO}_6$ with C2/m space group) and fully charged ($\text{NaNi}_2\text{BiO}_6$ with P-31 m space group) materials, the model structures obtained from the Rietveld refinements were used. The amplitude reduction factor (S_0^2) was determined to be 0.81 for Ni K-edge and 0.9 for Bi L₃-edge from the preliminary fitting sessions, and then fixed during the final fitting. Only single scattering path was considered during the fitting of all spectra.

1) Ni K-edge EXAFS

The filtered FTs of the EXAFS spectra in a R range of 1.1 ~ 3.1 \AA covering the first Ni-O and second Ni-M shells were fitted. The coordination numbers are fixed as determined from the model structure except for the first Ni-O shell with the halfway charged and fully charged states to take the Jahn-Teller distortion effect into account. The same inner shell potential shift (ΔE) was shared for all of the paths while the separate fitting parameters of the bond distance (R) and Debye-Waller factor (i.e., mean square disorder, σ^2) were used for each shell. In order to reduce the fitting variables, averaged Ni-O₆ bond length and single σ^2 were employed of the first Ni-O shell, which results in acceptable fitting quality. In case of the halfway- and fully- charged states, two Ni-O shells with varying coordination numbers were considered to take Jahn-Teller distortion effect into account while the sum of the coordination numbers constrained to be 6.

2) Bi L₃-edge EXAFS

The filtered FTs of the EXAFS spectra in a R range of 1.1 ~ 3.1 Å covering the first Bi-O and second Bi-Ni shells were fitted. The coordination numbers are fixed as determined from the model structure used. The same inner shell potential shift (ΔE) was shared for all of the paths while the separate fitting parameters of the bond distance (R) and Debye-Waller factor (i.e., mean square disorder, σ^2) were used for each shell.